Statistical properties of complex states of $^{67}_{30}$Zn

J. B. Garg and V. K. Tikku
State University of New York, Albany, New York 12222

J. A. Harvey, R. L. Macklin, and J. Halperin
Oak Ridge National Laboratory, Oak Ridge, Tennessee 37830

(Received 16 March 1981)

High resolution neutron total and capture cross section measurements have been made on the separated isotope ^{66}Zn in the energy range from a few keV to about 1 MeV using the neutron time-of-flight technique and the pulsed Oak Ridge Electron Linear Accelerator. The nominal resolution of the measurements was 0.07 ns/m. The total cross section data have been analyzed up to 380 keV using a multilevel R-matrix formalism and the capture data up to 130 keV using a least squares fit program. From these analyses we have obtained the values of the resonance parameters E_0, $g\Gamma_n$, and Γ_γ, and values of average quantities: $D_{l=0} = (4.62 \pm 0.55)$ keV, $D_{l=1} = (1.17 \pm 0.14)$ keV, $S_0 = (2.06 \pm 0.36)$, $S_1 = (0.66 \pm 0.06)$, and $S_2 = (0.50 \pm 0.12)$ in units of 10^{-4} eV$^{-1/2}$. The values of average radiation widths are (0.39 ± 0.06) eV for s-wave resonances and (0.190 ± 0.013) eV for p-wave resonances. The distributions of neutron reduced widths and of level spacings of s- and p-wave resonances show excellent agreement with the Porter-Thomas and Wigner distributions, respectively. The value of the Δ_3 statistic for the long range correlation of s-wave energy levels is found to be in reasonable agreement with the theoretical prediction of Dyson and Mehta. A value of 0.59 ± 0.10 has been determined for the linear coefficient for the correlation between the neutron reduced widths and the radiation widths of 26 s-wave resonances. This value is highly significant and has a confidence level of 99.7%.

[NUCLEAR REACTIONS ^{66}Zn(n,n), ^{66}Zn(n,γ), E = few keV to ~380 keV. Measured total and capture cross sections versus neutron energy, deduced resonance parameters, E_0, J^π, $g\Gamma_n$, Γ_γ, S_0, S_1, S_2, D_0, D_1.]

INTRODUCTION

This paper reports the results of high resolution neutron total and capture cross section measurements on the isotope ^{66}Zn. Such high resolution measurements in the past have provided great insight into the nature of neutron interactions with nuclei by the determination of the variations of neutron strength functions vs atomic mass[1] and the presence of doorway states[2] in some nuclei. In addition, the predictions of various statistical theories for such quantities as level spacings[3] and reduced neutron width distributions[4] of compound states have been tested to greater and greater accuracies.[5] It has been emphasized[6] recently that in order to test these theories it is absolutely essential to ascertain accurate J^π assignments of resonances and to make certain that no resonances have been missed in the data. This stringent requirement can be essentially fulfilled in many cases by careful measurements of both the total and capture cross sections of the same nuclide. The previous information on the parameters of the isotope ^{66}Zn has been mainly obtained from measurements[7] either on samples of natural zinc which consists of many isotopes or up to only a few keV for separated isotopes. Hence, these earlier measurements are not sufficient to test these theoretical predictions.

Also, measurements of average capture cross sections provide useful data for reactor shielding and nucleosynthesis applications. Thus, the present measurements fill the existing gap of precise information on these nuclear properties in this mass region.

EXPERIMENTAL DETAILS OF TOTAL CROSS SECTION MEASUREMENTS

These cross section measurements were made with ORELA, which is one of the few laboratories in the world capable of making high resolution neutron measurements in the keV energy range. For the total cross section measurements a flight path of 78.203 meters was chosen. The channel widths of the time-of-flight analyzer were varied from 1 ns to 32 ns over the energy interval from 1 MeV to about 30 eV, respectively. The electron pulse width was 5 ns at a repetition rate of 800 Hz. The overall time resolution of the spectrometer was about 0.07 ns/m at the highest neutron energy. The isotope of ^{66}Zn was in the form of ZnO and its isotopic enrichment is given in

Table I. Measurements were made for a sample enriched in ^{66}Zn with an inverse thickness 1/n of 12.89 b/atom of Zn. Since this sample is too thick for the determination of peak cross sections of the low energy resonances, measurements were also made using natural zinc samples with inverse thicknesses of 75 and 300 b/atom. For measurements above about 10 keV the neutron detector was a NE 110 fast scintillator mounted on a 5" diam RCA 4522 photomultiplier. For the low energy region below 20 keV a ^{6}Li-glass scintillation detector was used. Samples of ^{238}U and polyethylene were also used during these measurements for the determination of background. The details of the experimental arrangement are given in a previous publication.[8] The accelerator running time was about two days.

TABLE I. Atomic percent abundance of zinc isotopes in the ^{66}Zn sample used.

Mass number	64	66	67	68	70
% abundance	0.35	99.35	0.12	0.19	<0.05

ANALYSIS OF TOTAL CROSS SECTION DATA

The data for open beam and with samples in position were corrected for dead time and background in a manner discussed in an earlier publication.[8] The transmissions of the oxide samples were corrected for the oxygen content. The final cross section data were analyzed with a multilevel R-matrix formalism in the energy range from

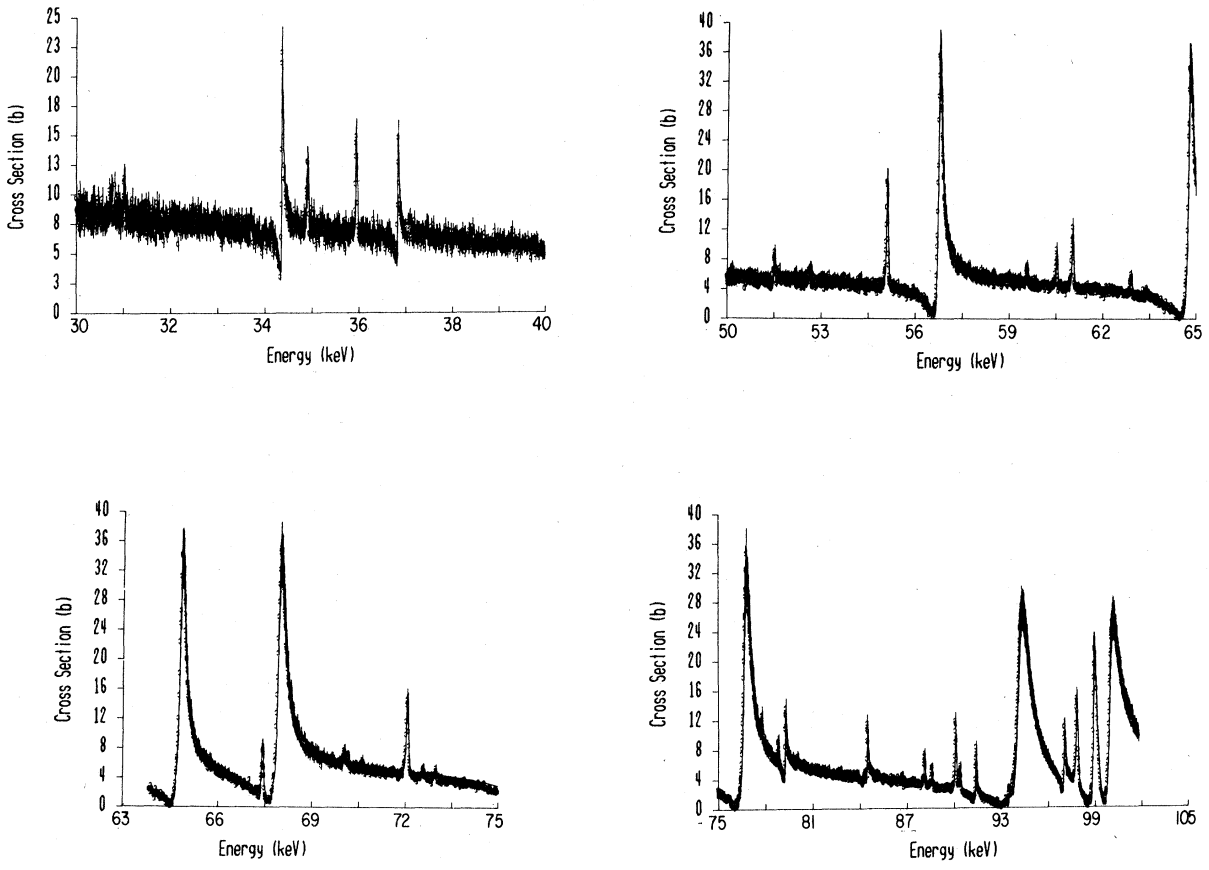

FIG. 1. The total cross section data for the ^{66}Zn nucleus in the neutron energy range from 30 to 102 keV. The solid curves are the theoretical cross section values obtained from a R-matrix multi-level analysis. The solid curves are slightly off center from the experimental data points (circles) due to improper alignment of the calcomp plotter.

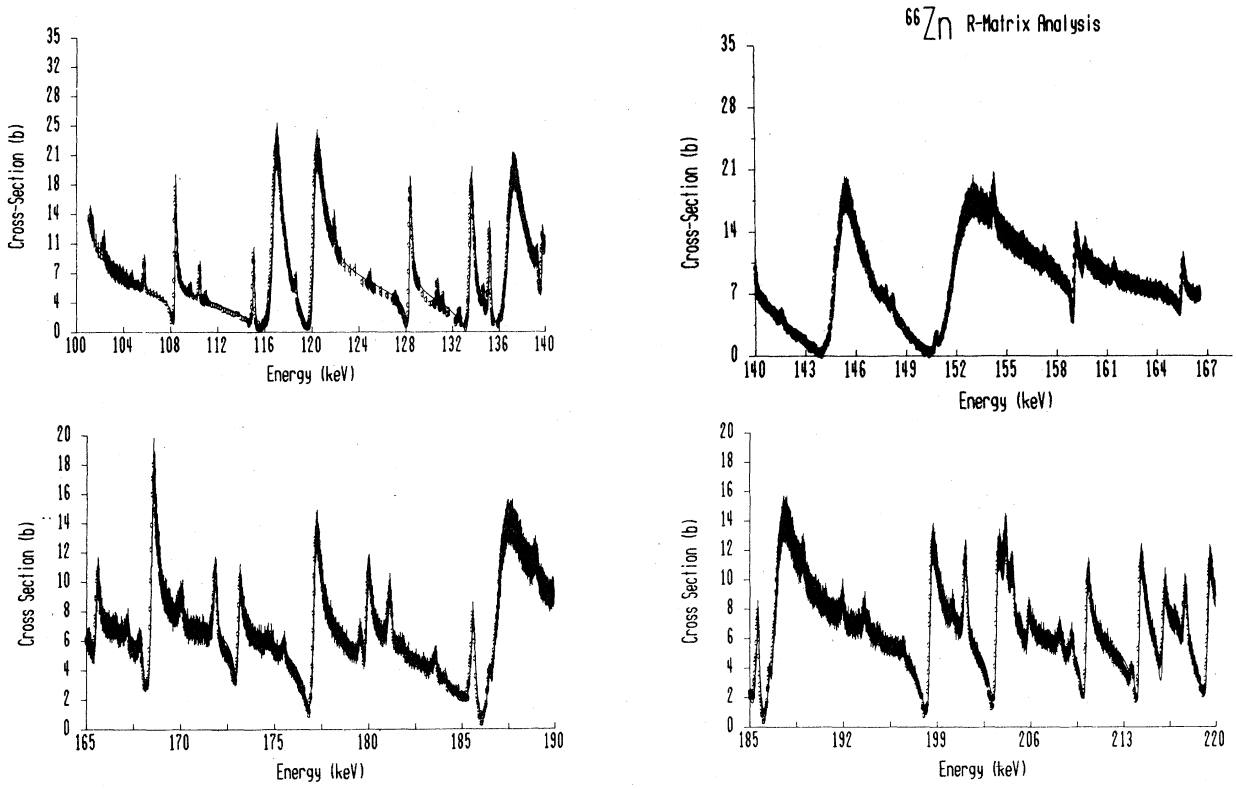

FIG. 2. The neutron total cross section data for ^{66}Zn from 101 to 220 keV. The solid curves are the theoretical R-matrix fit. The same comments as in Fig. 1 apply.

100 eV to about 380 keV. The resonance structure above about 300 keV becomes rather complex and accurate values of the neutron widths above this energy are not assured. Hence, for an investigation of the statistical properties of ^{66}Zn we have confined the analysis to a maximum energy of 300 keV.

The experimental cross section data (points) with the R-matrix multilevel fits (solid lines) from 30 to 102 keV, 101 to 220 keV and 220 to 380 keV are shown in Figs. 1, 2 and 3, respectively. The theoretical fit to the data is excellent except for two isolated energy regions between 128 and 132 keV, between 276 and 280 keV. In both of these regions the theoretical cross sections are slightly larger than the experimental data. The reason for this discrepancy is not understood. The figures show many asymmetrical s-wave resonances and nearly symmetrical p-wave resonances. The superposition of narrow resonances on broad s-wave resonances introduces large uncertainties in the determination of neutron widths of the narrow resonances. These resonances with small Γ_n are observed better in the capture cross section measurements in view of their comparable or larger Γ_γ values.

Assuming that the average reduced neutron width does not depend on the neutron energy, $\overline{\Gamma_n}$ for s-wave resonances varies as $\sqrt{E_n}$, whereas the resolution width of the spectrometer, which varies as E_n to $E_n^{1.5}$, increases much faster. Since the observation of narrow resonances depends upon the instrumental resolution, the threshold for the detection of weak resonances varies as a function of neutron energy. We have estimated this threshold for the total cross section measurement for the sample thickness used. We feel that we can clearly observe resonances with minimum neutron widths as given in Table II. However, resonances with values of $g\Gamma_n$ lower than these are observed, but the uncertainties in their widths are large. Thus, it is better to obtain values of $g\Gamma_n$ for these very weak resonances from the capture data by using an assumed value of Γ_γ.

The final values of E_o, $g\Gamma_n$ and the associated uncertainties for s- and p-wave resonances as obtained from both the transmission and capture measurements are given in Tables III, IV, V and VI.

EXPERIMENTAL ARRANGEMENT FOR THE CAPTURE CROSS SECTION MEASUREMENTS

These measurements were made at the 40 m station of the Oak Ridge Electron Linear

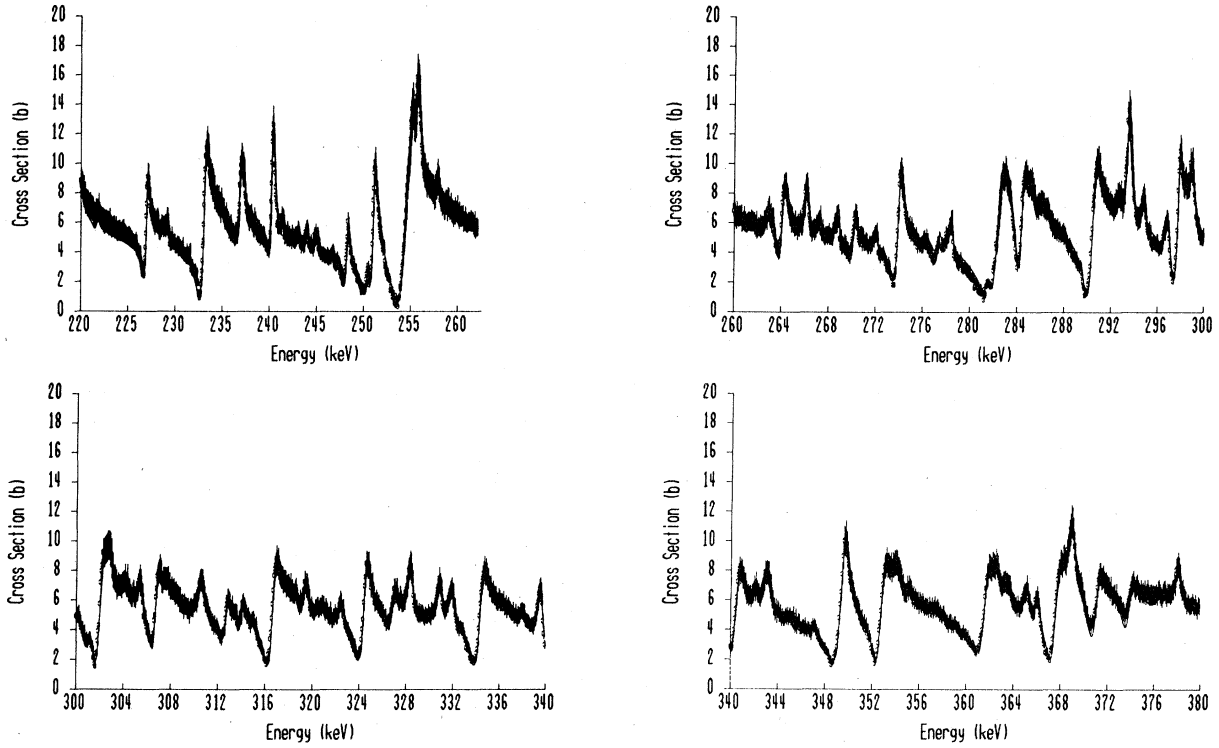

FIG. 3. The neutron total cross section data for ^{66}Zn from 220 to 380 keV. The solid curves are the theoretical R-matrix fit. Similar comments made in Fig. 1 also apply here.

Accelerator with similar conditions of pulse width and the repetition rate as in the transmission measurements. A sample of ZnO enriched in ^{66}Zn with percent abundance as given in Table I and weighing 6.91 g was in the form of a circular disk approximately 1.3 cm radius and 0.6 cm thick. The sample was placed between a pair of total

TABLE II. Minimum values of neutron widths for which a resonance in a given energy range can be experimentally observed in the transmission measurements for the sample thickness used in these measurements. Column 5 gives the percentage loss of levels in each energy interval due to sensitivity based on the Porter-Thomas distribution. Column 6 gives the number of observed levels and column 7 gives the total number of levels missed in each 100 keV energy interval.

E_n (keV)	$g\Gamma_n$(eV)	$g\Gamma_n^o$(eV)	$X=(\Gamma_n^o/\langle\Gamma_n^o\rangle)$ for $g\langle\Gamma_n^o\rangle=1$ eV	% Loss of levels from X=0 to X	No. of observed levels	Total loss of levels
10-19	0.1	~ 0.001	1×10^{-3}	2.5	3	
20-39	0.15	~ 0.001	1×10^{-3}	2.5	5	
40-59	0.3	~ 0.0015	1.5×10^{-3}	3.0	5	0.7
60-79	0.5	~ 0.002	2×10^{-3}	3.5	4	
80-99	0.8	~ 0.003	3×10^{-3}	4.2	5	
100-129	1.0	~ 0.003	3×10^{-3}	4.2	5	
130-159	2.0	~ 0.0035	3.5×10^{-3}	4.5	6	1.0
160-199	3.0	~ 0.0076	7.6×10^{-3}	6.7	8	
200-249	4.0	~ 0.0088	8.8×10^{-3}	7.1	11	1.7
250-299	5.0	~ 0.010	1.0×10^{-2}	7.6	12	
300-349	15.	~ 0.027	2.7×10^{-2}	12	10	2.0
350-369	25.	~ 0.042	4.2×10^{-2}	15	5	

TABLE III. The parameters of s-wave resonances as obtained from the R-matrix analysis of the total cross section data. The third column gives the capture area as obtained from LSFIT analysis of the capture data. The last column gives the Γ_γ after correction for k has been made. The levels marked with * have doubtful parity assignments.

E_o(keV)	ΔE_o(eV)	Γ_n(eV)	$\frac{g\Gamma_n(\Gamma_\gamma+k\Gamma_n)}{\Gamma}$ (meV)	$\Gamma_\gamma+k\Gamma_n$ (meV)	Γ_γ(meV)
4.046	± 2	5.2 ± 0.5	194.6 ± 1.8	202 ± 2	198 ± 2
10.420	± 5	112. ± 5	470.7 ± 6.9	473 ± 7	419 ± 7
14.200	± 5	570. ± 30	1998.8 ± 29.2	2006 ± 29	1772 ± 25
17.040	± 6	4.2 ± 0.5	292.6 ± 5.2	314 ± 6	312 ± 6
19.520	± 6	289 ± 15	554.0 ± 11.9	555 ± 12	448 ± 12
24.310	± 10	436 ± 20	717.8 ± 20.7	719 ± 21	551 ± 21
31.020	± 10*	0.72 ± 0.10	113.6 ± 4.5	133 ± 10	133 ± 10
34.380	± 10	8.20 ± 0.7	221.9 ± 7.3	229 ± 8	225 ± 8
36.845	± 10	4.3 ± 0.3	142.8 ± 0.3	148 ± 7	147 ± 7
42.640	± 15	176 ± 10	457.1 ± 17.6	458 ± 18	397 ± 18
44.990	± 15	15 ± 3	427.0 ± 13.7	438 ± 14	431 ± 14
51.516	± 15	4 ± 1	458.3 ± 20.1	518 ± 18	517 ± 18
56.762	± 15	98 ± 5	295.9 ± 17.8	297 ± 18	267 ± 18
59.580	± 15*	2 ± 0.2	274 ± 12.6	317 ± 12	317 ± 12
64.790	± 15	160 ± 8	372.7 ± 20.5	374 ± 21	335 ± 21
67.930	± 15	173 ± 10	487.8 ± 73.4	489 ± 74	447 ± 74
76.728	± 20	400 ± 20	779.0 ± 36.0	781 ± 36	687 ± 36
79.265	± 20	11 ± 1	132.7 ± 28.4	134 ± 28	131 ± 28
84.485	± 20	14 ± 1	809.2 ± 40.1	858 ± 40	854 ± 40
91.400	± 20	14 ± 1	417.9 ± 32.3	430 ± 34	427 ± 34
94.255	± 20	660 ± 35	535.6 ± 80.1	536 ± 80	298 ± 50
97.045	± 20	20 ± 2	318.1 ± 23.6	323 ± 25	319 ± 30
98.977	± 20	215 ± 10	273.4 ± 36.2	274 ± 36	193 ± 36
100.053	± 25	565 ± 30	720 ± 100	721 ± 100	511 ± 72
108.391	± 25	89 ± 5	626.4 ± 44.6	631 ± 45	599 ± 40
116.818	± 25	855 ± 50	707.1 ± 86.5	708 ± 87	439 ± 60
120.277	± 25	746 ± 40	534.4 ± 117.3	535 ± 118	293 ± 80
128.358	± 25	151 ± 8	888.2 ± 50.9	894 ± 52	853 ± 52

TABLE IV. The parameters of s-wave resonances as obtained from the R-matrix analysis of total cross section data. The level marked with * has a doubtful parity assignment but this one is favored.

E_o (eV)	ΔE_o (eV)	Γ_n (eV)	$\Delta\Gamma_n$ (eV)	E_o (eV)	ΔE_o (eV)	Γ_n (eV)	$\Delta\Gamma_n$ (eV)
133575	25	347	20	254320	50	1500	100
136901	25	1258	100	262365	50	21	3
139717	25	39	4	263965	50	80	5
144945	30	1218	100	270080	50	70	5
152040	30	2768	200	274000	50	310	10
159071	30	73	5	277230	55	45	15
165475	35	46	5	282289	55	1500	300
168415	35	197	10	284310	55	435	200
173082	35	62	5	285750	55	28	3
177088	35	264	15	290305	55	700	100
179890	35	66	5	297630	55	260	60
186947	40	1352	100	301910	60	680	60
194485*	40	7	1	306630	60	250	20
198490	40	423	25	312632	60	110	10
203441	40	338	32	313920	60	60	5
205763	40	21	3	316542	60	485	20
210171	40	172	12	324299	60	300	20
214184	40	301	150	326700	60	96	10
215965	40	142	20	334230	60	515	20
219365	40	360	20	340295	60	265	50
226940	40	171	10	349146	60	620	30
233044	45	540	20	352593	65	475	25
236757	45	124	10	361325	65	650	50
240161	45	85	10	367375	65	400	40
248200	45	87	10	370950	65	305	30
250970	50	550	20	373780	65	162	20

energy γ-ray detectors. The neutron beam was collimated to irradiate the sample while avoiding the detectors. The details of the experimental arrangement and these detectors have been given previously.[9] The curves of the measured capture cross section vs neutron energy up to 900 keV are shown in Figs. 4, 5 and 6.

ANALYSIS OF CAPTURE CROSS SECTION DATA

The LSFIT program[10] gives the thin sample observed area $A_\gamma = 2\pi^2\lambda\bar{}^2 g\Gamma_n\Gamma_\gamma'/\Gamma$, and the kernel of this area $g\Gamma_n\Gamma_\gamma'/\Gamma$ is given in Tables III and V for s- and p-wave resonances, respectively. The Γ_γ' is the measured radiation width modified from the real value by the neutron sensitivity factor k for elastically scattered neutrons. The value of k as a function of neutron energy has been measured for the isotopes of zinc using a procedure described by Allen et al.[11] In order to obtain the value of Γ_γ, this correction is applied by the relation $\Gamma_\gamma = \Gamma_\gamma' - k\Gamma_n$. The correction is obviously important for broad resonances ($\Gamma_n \gtrsim 100$ eV) but almost negligible for narrow resonances ($\Gamma_n \lesssim 10$ eV). From the measured capture area one can determine the value of Γ_γ or Γ_n if the other quantity and

TABLE V. The parameters of $\ell>0$ resonances obtained from the total and capture cross section data. The second column gives the capture area obtained from the LSFIT analysis. The last column gives the d-wave probability. The resonances marked with * are most likely doublets. The value g = 1 has been assumed except where g = 2 is required for a good fit. If a value of Γ_γ = 170 meV is indicated, it means that the $g\Gamma_n$ value and its uncertainty were determined from the capture data. The value of Γ_γ for which an uncertainty is quoted is determined for an assumed value of g and the value of $g\Gamma_n$ obtained from the transmission data. No value of Γ_γ is calculated for resonances which are assumed doublets.

E_o(keV)	$\frac{g\Gamma_n(\Gamma_\gamma+k\Gamma_n)}{\Gamma}$ (meV)	$g\Gamma_n$(eV)	Γ_γ(meV)	g	P(d)
3.558	5.79 ± 0.18	0.0060 ± 0.0002	170	1	
4.385	49.27 ± 0.64	0.072 ± 0.012	156 ± 25	1	
5.204	2.04 ± 0.19	0.0021 ± 0.0002	170	1	
5.343	85.10 ± 0.77	0.15 ± 0.02	206 ± 25	1	
6.482	2.82 ± 0.55	0.0030 ± 0.0005	170	1	
6.714	138.05 ± 9.9	0.20 ± 0.02	222 ± 25	2	
8.950	3.06 ± 0.42	0.0030 ± 0.0006	170	2	50
9.175	99.49 ± 1.27	0.18 ± 0.04	223 ± 25	1	
9.816	133.52 ± 1.46	0.24 ± 0.04	144 ± 18	2	
10.886	116.38 ± 1.37	0.18 ± 0.04	170	2	
13.275	6.49 ± 1.04	0.007 ± 0.002	170	2	53
13.414	33.57 ± 1.56	0.042 ± 0.002	170	1	
15.632	216.15 ± 3.19	0.60 ± 0.10	170 ± 15	2	
15.880	27.77 ± 1.59	0.033 ± 0.003	170	1	
17.260	245.03 ± 4.14	1.55 ± 0.15	291 ± 10	1	
17.350	11.42 ± 1.53	0.012 ± 0.002	170	2	60
20.726	50.44 ± 1.89	0.072 ± 0.004	170	1	
20.815	114.41 ± 2.39	0.35 ± 0.03	170 ± 10	1	
21.680	33.88 ± 3.31	0.042 ± 0.005	170	1	
21.705	276.71 ± 5.49	5.0 ± 0.3	146 ± 8	2	
23.076	28.69 ± 1.92	0.035 ± 0.003	170	1	
24.078	242.76 ± 6.54	4.25 ± 0.43	258 ± 10	1	
24.617	18.39 ± 3.12	0.019 ± 0.004	170	2	78
25.995	24.20 ± 2.66	0.026 ± 0.004	170	2	69
26.433	52.69 ± 3.36	0.075 ± 0.004	170	1	
26.690	186.21 ± 4.80	0.86 ± 0.07	119 ± 9	2	
27.387	82.42 ± 3.33	0.16 ± 0.02	170	1	
28.523	3.44 ± 2.24	0.004 ± 0.002	170	2	95
28.864	17.89 ± 2.92	0.019 ± 0.004	170	2	86
29.017	39.72 ± 3.36	0.045 ± 0.007	170	2	50
29.340	201.58 ± 5.46	0.5 ± 0.1	170 ± 25	2	
33.730	142.25 ± 5.30	0.24 ± 0.01	170	2	
34.920	257.23 ± 7.11	1.2 ± 0.2	164 ± 12	2	
35.169	27.63 ± 4.04	0.030 ± 0.006	170	2	85
35.960	150.91 ± 6.23	2.1 ± 0.1	163 ± 7	1	
37.480	150.49 ± 7.32	0.27 ± 0.02	170	2	
37.840	64.86 ± 5.03	0.10 ± 0.01	170	1	
40.370	162.98 ± 7.35	4.0 ± 0.2	170 ± 8	1	
40.570	253.39 ± 8.03	2.4 ± 0.1	283 ± 15	1	
40.715	145.81 ± 6.02	0.24 ± 0.02	170	2	
41.260	80.33 ± 6.11	0.15 ± 0.02	170	1	
41.840	270.87 ± 9.06	2.4 ± 0.1	153 ± 6	2	
43.650	251.41 ± 8.71	8.4 ± 0.4	129 ± 5	2	
45.882*	453.29 ± 12.47	0.36 ± 0.10		2	
46.175	45.82 ± 9.35	0.053 ± 0.018	170	2	83
46.225	207.51 ± 10.89	0.36 ± 0.10	233 ± 35	2	
46.708	103.95 ± 5.29	0.150 ± 0.010	170	2	
48.485	215.04 ± 8.53	0.80 ± 0.20	148 ± 12	2	
49.045*	298.00 ± 10.88	0.20 ± 0.06		2	
49.790	416.41 ± 14.96	12.4 ± 0.6	215 ± 8	2	
51.415*	214.42 ± 12.96	0.18 ± 0.08		2	51
51.685	60.58 ± 7.97	0.074 ± 0.001	170	2	80
52.024	100.16 ± 8.50	0.24 ± 0.05	170	1	
52.670	291.92 ± 12.49	1.5 ± 0.3	182 ± 20	2	
53.142	42.79 ± 8.08	0.049 ± 0.012	170	2	88
53.332	85.07 ± 8.11	0.114 ± 0.023	170	2	75

TABLE V. *(Continued.)*

E_0(keV)	$\frac{g\Gamma_n(\Gamma_\gamma+k\Gamma_n)}{\Gamma}$ (meV)	$g\Gamma_n$(eV)	Γ_γ(meV)	g	P(d)
53.789	75.83 ± 5.74	0.098 ± 0.015	170	2	80
54.934	78.24 ± 8.89	0.10 ± 0.02	170	2	81
55.040		0.45 ± 0.12		2	
55.110	268.43 ± 12.44	26.4 ± 1.25	137 ± 6	2	
55.967		0.53 ± 0.15		2	
57.610	56.72 ± 9.63	0.068 ± 0.017	170	2	88
57.745*	337.53 ± 15.49	0.55 ± 0.08		2	
58.500	166.44 ± 12.15	0.30 ± 0.06	170	2	
60.530	165.27 ± 11.04	4.6 ± 0.2	172 ± 12	1	
61.040	300.70 ± 13.47	10.8 ± 0.5	155 ± 8	2	
61.800	61.69 ± 6.72	0.075 ± 0.010	170	2	88
62.915	334.54 ± 14.42	2.5 ± 0.1	192 ± 8	2	
63.411	161.56 ± 10.46	0.54 ± 0.10	228 ± 25	1	
63.635	237.72 ± 12.29	1.0 ± 0.2	156 ± 22	2	
65.554	118.59 ± 8.59	0.18 ± 0.02	170	2	75
65.987	41.74 ± 7.47	0.048 ± 0.012	170	2	91
67.428	379.43 ± 39.53	12.0 ± 0.6	195 ± 22	2	
67.735	66.40 ± 32.12	0.083 ± 0.05	170	2	88
67.785	62.25 ± 35.74	0.076 ± 0.05	170	2	89
68.318		3.0 ± 0.60		2	
69.109	172.46 ± 31.19	0.50 ± 0.12	263 ± 73	1	
69.896	132.96 ± 31.17	1.3 ± 0.1	149 ± 39	1	
70.040	79.50 ± 35.98	2.6 ± 0.6	82 ± 30	1	
70.150	300.73 ± 42.35	1.6 ± 0.2	185 ± 25	2	
70.620*	464.58 ± 44.61	1.5 ± 0.5		2	
71.135	222.55 ± 40.53	0.4 ± 0.1	170	2	
71.952		0.62 ± 0.15		2	
72.050	174.37 ± 48.81	25.2 ± 2.0	89 ± 50	2	
72.580	228.30 ± 50.80	0.70 ± 0.15	169 ± 20	2	
72.985	352.76 ± 57.01	0.68 ± 0.15	362 ± 55	2	
75.473	169.77 ± 14.09	0.34 ± 0.06	170	2	61
75.720	274.03 ± 16.17	0.50 ± 0.06	170	2	
77.162	40.02 ± 16.94	0.045 ± 0.029	170	2	91
77.300*	418.30 ± 23.86	3.0 ± 0.3		2	
77.807	159.91 ± 14.29	5.6 ± 0.4	164 ± 16	1	
78.430	155.91 ± 16.57	0.28 ± 0.03	170	2	75
78.830	122.90 ± 14.13	4.6 ± 0.2	126 ± 16	1	
79.113	21.79 ± 13.50	0.023 ± 0.013	170	2	92
79.315	102.07 ± 28.98	0.15 ± 0.06	170	2	86
79.515	27.79 ± 12.76	0.030 ± 0.012	170	2	92
79.960	28.52 ± 13.47	0.031 ± 0.012	170	2	92
80.080	332.90 ± 18.47	0.8 ± 0.2	282 ± 15	2	
81.710*	344.19 ± 19.80	2.0 ± 0.2		2	
82.910	169.16 ± 18.33	0.34 ± 0.10	170	2	72
83.605	161.19 ± 19.93	0.28 ± 0.10	188 ± 30	2	78
83.924*	488.47 ± 31.63	0.85 ± 0.10		2	
84.370	115.53 ± 15.85	0.18 ± 0.06	170 ± 10	2	85
85.321	252.34 ± 25.09	0.60 ± 0.15		2	
86.750*	577.39 ± 33.33	1.0 ± 0.2		2	
88.157	152.52 ± 21.33	6.0 ± 0.6	157 ± 24	1	
88.627	286.33 ± 25.22	3.0 ± 0.3	158 ± 16	2	
89.700*	476.19 ± 35.27	10.0 ± 1.0		2	
90.140	235.18 ± 25.23	26.6 ± 2.5	237 ± 26	1	
90.422	122.50 ± 14.69	5.2 ± 0.5	126 ± 15	1	
93.304*	179.64 ± 20.05	0.36 ± 0.10	170	2	78
93.550	164.69 ± 21.72	3.0 ± 0.3	174 ± 24	1	
94.430	382.29 ± 33.43	2.0 ± 0.3	236 ± 29	2	
96.275	82.68 ± 17.68	0.11 ± 0.04	170	2	90
97.150*	234.85 ± 27.15	1.0 ± 0.2		2	
97.460*	389.43 ± 30.61	10.4 ± 1.0		2	
97.880	111.71 ± 20.20	56.0 ± 5.0	112 ± 20	1	
99.715	381.82 ± 40.89	2.0 ± 0.3	236 ± 35	2	
100.410	211.32 ± 27.77	10.0 ± 1.0	216 ± 29	1	
101.430	395.07 ± 42.07	2.0 ± 0.3	246 ± 33	2	
101.530	119.54 ± 27.88	0.18 ± 0.05	170	2	87

TABLE V. *(Continued.)*

E_o(keV)	$\frac{g\Gamma_n(\Gamma_\gamma+k\Gamma_n)}{\Gamma}$ (meV)	$g\Gamma_n$(eV)	Γ_γ(meV)	g	P(d)
102.340	211.64 ± 24.10	15.1 ± 1.5	215 ± 25	1	
103.620	110.69 ± 23.94	1.0 ± 0.2	123 ± 25	1	
103.800	125.53 ± 17.29	0.20 ± 0.03	170	2	87
103.960	201.88 ± 25.48	2.7 ± 0.3	217 ± 30	1	
104.720	376.05 ± 27.19	3.0 ± 0.3	214 ± 27	2	
105.550*	389.15 ± 31.18	4.0 ± 0.5		2	
105.790	226.20 ± 29.36	13.7 ± 1.0	230 ± 30	1	
107.580	483.22 ± 33.13	1.17 ± 0.20	412 ± 29	2	
108.572	149.09 ± 9.88	1.21 ± 0.65	170 ± 17	1	
109.700	372.49 ± 26.18	2.9 ± 0.3	214 ± 30	2	
110.510	404.20 ± 32.85	28.0 ± 3.0	205 ± 17	2	
111.035	133.25 ± 23.58	2.0 ± 0.3	143 ± 27	1	
113.710	452.63 ± 30.91	2.0 ± 0.3	293 ± 26	2	
114.430	398.24 ± 32.22	2.0 ± 0.3	249 ± 25	2	
115.088	369.80 ± 33.18	45.0 ± 4.0	373 ± 34	1	
116.010	266.02 ± 28.14	1.3 ± 0.2	335 ± 32	1	
117.790	199.04 ± 26.78	1.0 ± 0.4	124 ± 42	2	60
118.650	319.11 ± 31.12	6.5 ± 0.6	167 ± 17	2	
120.120*	512.91 ± 47.83	1.2 ± 0.2			
120.800	96.19 ± 23.50	0.13 ± 0.05	170	2	90
121.170	272.63 ± 27.82	1.2 ± 0.2	172 ± 21	2	50
121.970	319.26 ± 31.46	6.1 ± 0.6	165 ± 17	2	
123.000*	503.35 ± 34.61	2.0 ± 0.3			
123.380	152.46 ± 7.34	0.28 ± 0.05	170	2	87
124.510*	424.48 ± 34.27	3.0 ± 0.4			
124.970	395.67 ± 32.70	1.2 ± 0.5	296 ± 21	2	54
125.550	265.15 ± 33.57	0.8 ± 0.4	198 ± 25	2	72
127.130	263.39 ± 39.13	3.0 ± 0.4	152 ± 30	2	
127.300	373.71 ± 47.85	5.8 ± 0.6	200 ± 30	2	
127.475	188.19 ± 36.31	0.42 ± 0.20	170	2	83
127.700	357.35 ± 32.88	4.2 ± 0.4	195 ± 30	2	
129.280	417.34 ± 33.47	20.0 ± 3.0	213 ± 33	2	

the g value of the resonance is known. The neutron widths of all the s-wave resonances and most of the broad p-wave resonances were determined from the total cross section measurements by use of an R-matrix multilevel fit. The calculated values of Γ'_γ and Γ_γ after correction for k are given in Tables III and V. The capture data (Figs. 4, 5 and 6) show well resolved resonances without overlap up to a neutron energy of about 50 keV, after which the resonances are still well resolved up to about 160 keV with occasional overlapping of resonances. The LSFIT[10] gives an accurate value of the capture area for isolated resonances and gives a fairly reasonable fit to the overlapping resonances. Up to about 50 keV 21 isolated p-wave resonances have been observed in the transmission measurements. Values of $g\Gamma_n$ determined for these resonances are given in Table V. For these resonances an average value of Γ_γ of 190 ± 13 meV has been obtained from this experiment. As mentioned earlier, for resonances whose $\Gamma_n \ll \Gamma_\gamma$, one can determine the $g\Gamma_n$ values if the Γ_γ value is known. For the very narrow resonances not observed in the transmission measurements we have assumed a value of Γ_γ = 170 meV. These values of $g\Gamma_n$ are also given in Table V. These values of $g\Gamma_n$ would be lower by ~ 10% if a value of Γ_γ of 190 meV were used for their determination. Since these narrow resonances contribute <10% to the p-wave strength function, this would result in a much smaller uncertainty in S_1 than that introduced by the finite size of the number of resonances.

RADIATION WIDTHS

Most of the values of Γ_γ for s-wave resonances (Table III) are larger than the values of Γ_γ for p-wave resonances (Table V). One notes that in general the larger the Γ_n, the larger the Γ_γ, which suggests that the correction for k is not adequate. We feel certain, however, that our k values are accurate to about 20-30% and, hence, this effect is genuine. The other convincing evidence is that the Γ_γ values are relatively small for some resonances such as at 56.762, 64.790, 94.255 and 98.977 keV, in spite of their large neutron widths.

One result does seem interesting and that is the radiation widths for s-wave resonances have a large spread in values, the smallest being 131 meV and the largest 1772 meV. Since the radiation width is the sum

TABLE VI. The parameters of $\ell>0$ resonances as obtained from the R-matrix analysis of the total cross section data.

E_o (eV)	$g\Gamma_n$ (eV)	E_o (eV)	$g\Gamma_n$ (eV)	E_o (eV)	$g\Gamma_n$ (eV)	E_o (eV)	$g\Gamma_n$ (eV)	E_o (eV)	$2g\Gamma_n$ (eV)	E_o (eV)	$2g\Gamma_n$ (eV)
130760	9	168220	15	204211	75	243970	44	294700	46	331802	139
131230	5	168580	39	204635	47	244820	23	296820	122	338024	21
131840	3	168891	10	208254	12	245120	16	297964	98	339560	210
132630	8	170045	15	209100	23	246720	20	298465	30	340850	76
133384	6	171845	50	213665	18	250490	73	298880	177	342075	95
134710	12	174632	7	216935	16	255285	155	300205	45	342905	159
135224	95	174930	3	217700	94	255800	309	301200	83	345100	22
136090	4	175520	8	219117	10	257930	49	302581	62	347120	22
136215	5	176926	10	221626	8	262920	30	304100	84	348855	36
136335	5	179600	28	221940	7	263180	32	304820	48	349718	184
139315	8	179780	14	225875	5	264350	60	305350	125	353256	112
139997	3	180065	39	226692	22	265600	15	307614	56	353930	154
141510	5	181150	40	227150	13	266060	98	310100	49	355151	48
144245	6	181708	7	228171	19	267200	26	310550	128	360640	57
144375	5	183555	7	228673	18	268575	27	313492	37	361060	57
144465	6	185400	18	229176	24	268850	19	314177	32	362000	57
147200	8	185610	101	231602	13	271980	24	315051	25	362580	92
147815	8	186144	4	232750	10	272680	5	318570	43	363445	98
148200	15	186360	7	234951	19	273600	15	319450	86	365078	125
150820	3	186460	32	236540	58	276100	21	320950	30	365978	87
154294	6	189010	28	237050	77	278310	73	321983	19	368200	146
157230	3	191943	30	237305	86	281530	52	322450	69	368880	410
159748	17	193600	18	238084	19	285203	22	324750	87	374260	24
161468	12	196500	8	240050	27	286585	24	326490	39	376370	60
166900	5	200230	16	240440	244	290900	65	327549	31	376980	60
167180	16	201138	115	241365	34	292715	106	328265	176	378000	216
167845	28	203170	8	243060	30	293500	352	330876	172	380425	169

of all partial radiation widths due to many transitions, they are expected to be nearly constant or follow a chi-squared distribution about the mean value with n degrees of freedom, where n represents the number of primary γ-ray transitions. From our data, if one discards the extremely large value of Γ_γ = 1772 meV from the s-wave population, one obtains a mean value of s-wave radiation width of (390 ± 60) meV. Here the uncertainty is calculated as $\Delta\Gamma_\gamma = \sigma/\sqrt{n-1}$ where σ is the standard deviation of the radiation width distribution assumed to be approximately normal, and n is the number of measured widths. A Monte Carlo analysis of the observed s-wave radiation width distribution gives a value of about 6 for the number of degrees of freedom of the chi-squared distribution.

A similar analysis of the 48 p-wave radiation widths measured in this experiment up to a neutron energy of 100 keV gives a value of Γ_γ of 190 ± 13 meV. A Monte Carlo analysis for the p-wave radiation width distribution gives ν = 24 for the number of degrees of freedom of this distribution. The difference between the mean radiation widths for s- and p-wave resonances is statistically significant and is related to the structure of the compound nucleus states as well as to the relative density of positive and negative parity low-lying excited states. The capture of s-wave neutrons populates positive parity states in the compound nucleus which would predominantly decay to the negative parity states via E1 transitions while the capture of p-wave neutrons would involve γ-ray transitions to the positive parity states. A similar effect was observed by us in the investigation[6] of the ^{64}Zn+n reaction.

UNCERTAINTIES IN THE RESONANCE PARAMETERS

The values of resonance parameters E_o, Γ_n, Γ_γ, etc., have associated uncertainties caused by numerous reasons. We have used least squares programs such as MULTI[12] for the analysis of total cross section and LSFIT[10] for the capture cross section. These programs generate uncertainties, based on the minimization of chi-squares for a given set of fitted parameters. These are in general much smaller (about 1%) than one would anticipate from the accuracy of the cross section data itself, which has an uncertainty of about 5% in the present measurements.

For the total cross section data, the accuracy of parameters depends upon the counting statistics, the instrumental resolution, background correction, normalization of data, etc. Similar problems exist in the capture data with an additional correction needed for self-shielding of γ rays and effects of neutron scattering

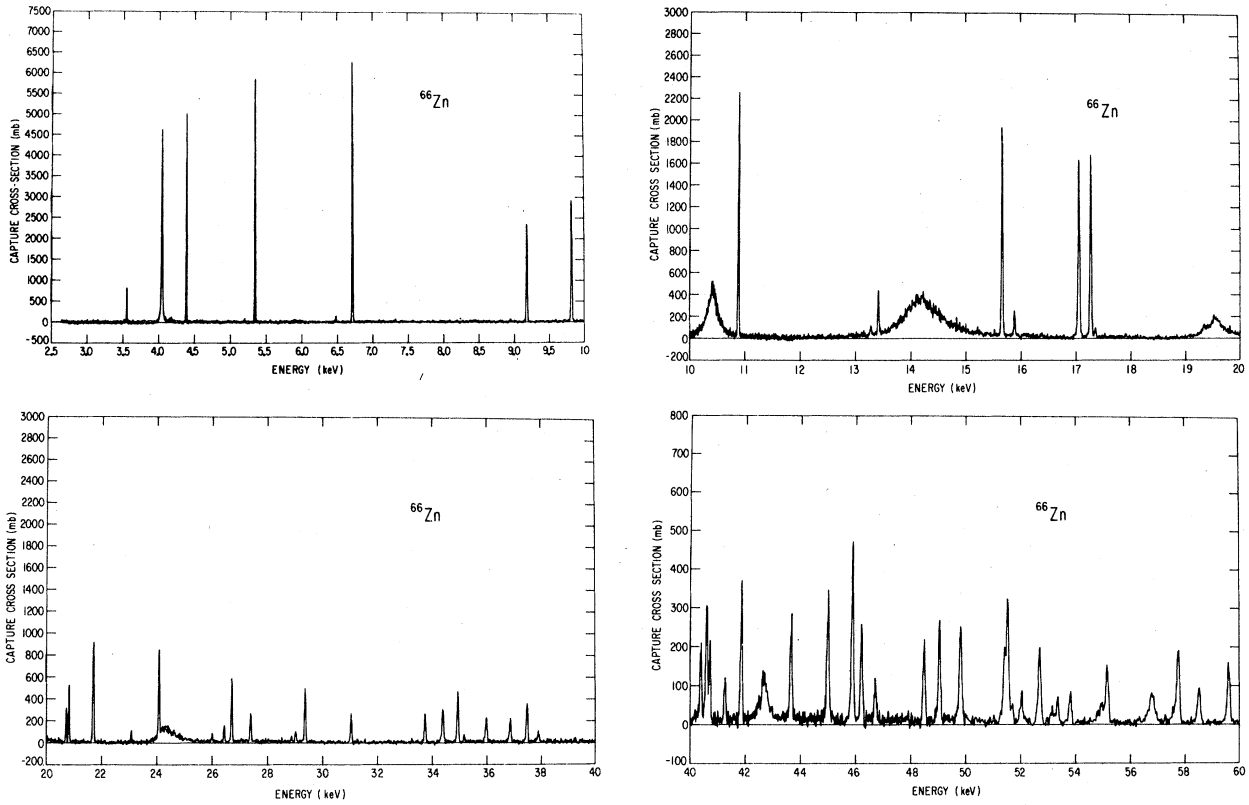

FIG. 4. The effective neutron capture cross section data for a thin oxide sample of enriched ^{66}Zn in the neutron energy range 2.5 to 60 keV. The solid curves merely connect the data points.

on the detectors. A detailed discussion of these uncertainties in resonance parameters is given below.

UNCERTAINTY IN E_o FROM THE TRANSMISSION DATA

The resonance energies given in Tables III and IV are the R-matrix eigenvalues which are somewhat lower than the energies where the cross sections are maxima. This behavior is typical only for s-wave resonances and arises from the interference between potential and resonance scattering, which gives an asymmetric shape to the resonance. The p-wave resonances have very small interference and, hence, the resonance energies occur at the peaks in the cross section. The uncertainty in the resonance energy is ~ 0.03% for broad s-wave resonances and somewhat smaller for narrow resonances. Any systematic error in the E_o values which may occur due to errors in the measurements of flight path and time zero are not included in the above estimates, but these are much smaller than those mentioned above.

We did find a small systematic difference of about 0.01% in resonance energies between the total and capture cross section measurements. Since the total cross section measurements were made at 78.2 m and the capture cross section measurements at 40 m, we have decided to use the energies obtained from the higher resolution transmission measurements.

UNCERTAINTIES IN THE NEUTRON WIDTHS OF RESONANCES

The MULTI-level program generates uncertainties of the parameters for an acceptable fit to the total cross section. In this analysis we have assumed a negative energy resonance below the energy region being analyzed and a positive energy resonance above it which have large neutron widths to produce the correct cross section between resonances. We have quoted uncertainties which take into account the effects of these negative and positive energy resonances in fitting the data. These uncertainties are more realistic than those generated by the program. For broad s-wave resonances, these uncertainties are in the neighborhood of 5% and for narrow resonances, where the effect of base line on the $g\Gamma_n$ values can be much more drastic we have found the uncertainties to be as large as 30%. One should, however, note that the uncertainties in the $g\Gamma_n$ values produce a smaller uncertainty in the strength function value than the uncer-

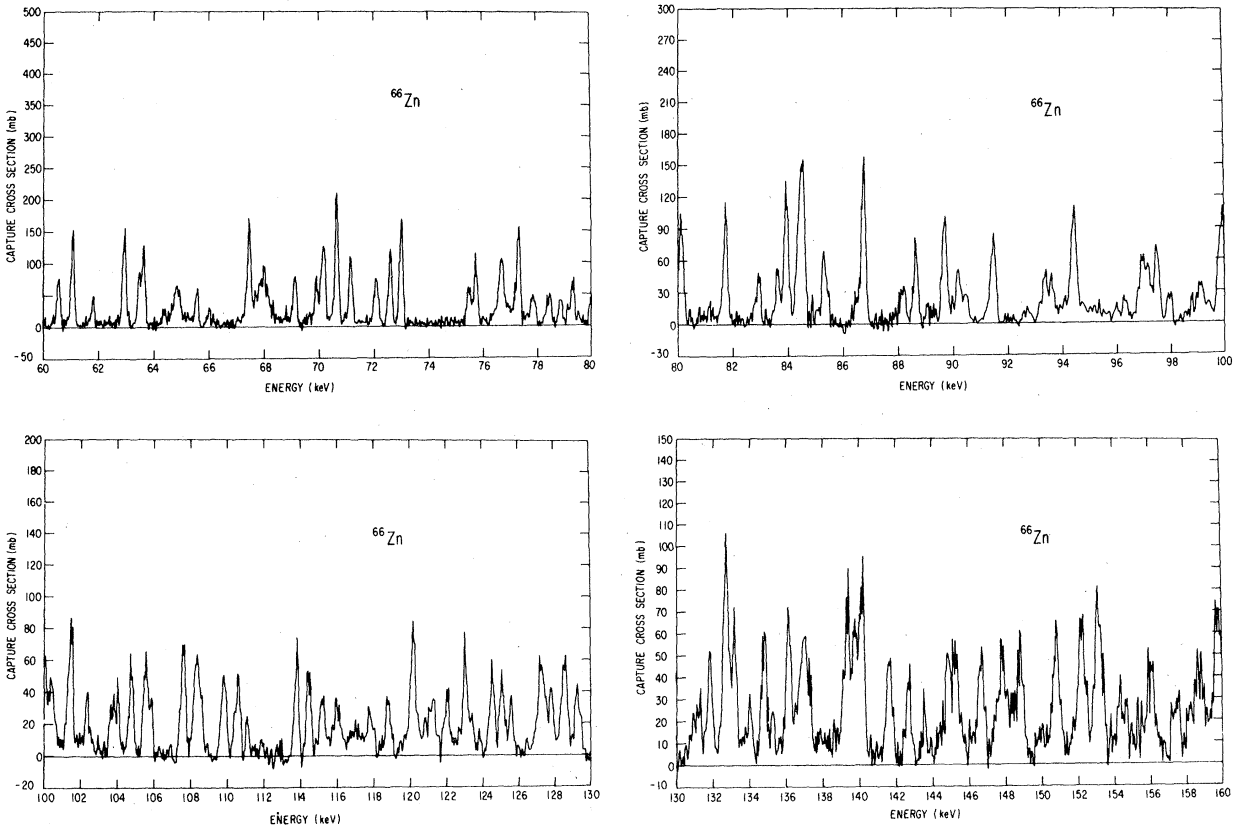

FIG. 5. The effective capture cross section data for ^{66}Zn from 60 to 160 keV.

tainty due to the limited number of resonances observed.

NEUTRON REDUCED WIDTH DISTRIBUTION FOR S-WAVE RESONANCES

Porter and Thomas[4] have predicted using the statistical arguments of the compound nucleus picture a wide variation in the neutron reduced widths of compound resonances. This distribution for the square roots of reduced widths (amplitudes) of a sequence of resonances of same J^{π} is given as

$$P(y)dy = (2/\pi)^{1/2} \exp\left(\frac{-y^2}{2}\right) dy$$

where

$$y = (\Gamma_n^o/\langle\Gamma_n^o\rangle)^{1/2} .$$

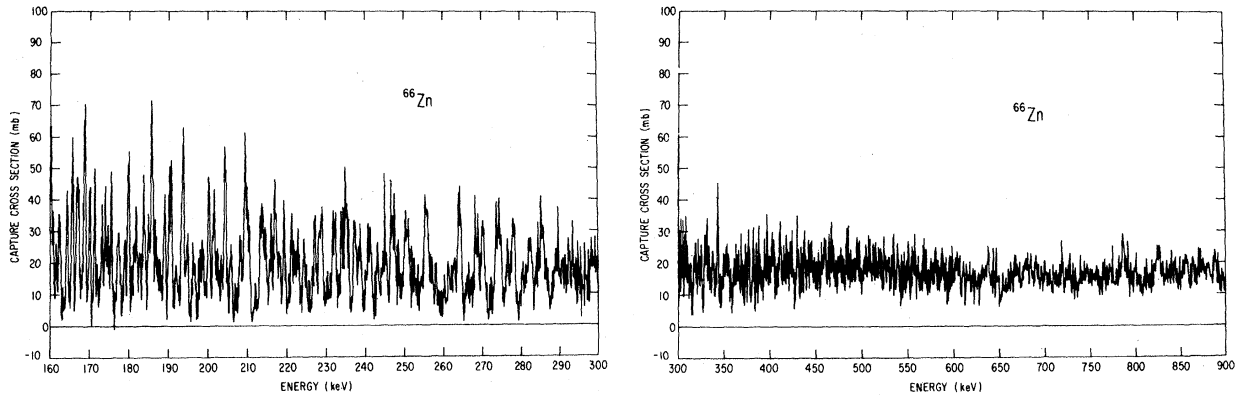

FIG. 6. The effective capture cross section data for ^{66}Zn in the energy interval 160 to 900 keV.

The calculated distribution for 64 s-wave resonances up to 300 keV is shown as a histogram in Fig. 7. We have also shown for comparison the theoretical Porter-Thomas distribution. In general the agreement between the two is quite good within the statistical uncertainty of the data. A more meaningful quantity is the numerical value of ν, the number of degrees of freedom of a chi-squared distribution. The results of a Monte Carlo calculation give a value for $\nu = 0.95^{+0.20}_{-0.23}$ in excellent agreement with the expected value of one for the Porter-Thomas distribution.

COMPARISON OF TRANSMISSION AND CAPTURE DATA

The transmission data show a single broad s-wave resonance at 24.310 keV, whereas a large p-wave resonance at 24.078 keV and a small p-wave resonance at 24.617 keV sitting on the shoulder of the s-wave resonance at 24.310 keV are seen in the capture data. This sensitivity of detecting narrow resonances in the capture measurements is absolutely essential for the determination of parameters of $\ell>0$ resonances.

A group of three resonances of comparable strength are observed in the capture cross section data between 48 and 50 keV, whereas in the transmission measurements we see only two resonances, a very weak one (Γ_n = 0.8 eV) and a large one (Γ_n = 12.4 eV). Similarly one observes a strong p-wave resonance at 81.7 keV in the capture but not in the transmission. The doublet at 84 keV is more clearly resolved in the capture data than in the transmission data. Between 68 and 76 keV there are 10 well resolved resonances in the capture, but in the transmission data there is one strong s-wave resonance, one p-wave resonance, and perhaps 4 more weak resonances. Between 100 and 130 keV at least 40 resolved resonances are observed in the capture data, while only 4 s-wave resonances, 8 p-wave resonances and perhaps 8 other narrow resonances are seen in the transmission data. In this energy region only about half of the narrow resonances can be ascertained in the transmission data. Thus, the sensitivity of the capture measurements for observing narrow resonances with $\Gamma_n \lesssim \Gamma_\gamma$ is essential. Most of the resonances in the capture cross section below 130 keV are well resolved; however, above about 130 keV resonances are not sufficiently resolved to give reasonably accurate values of the capture area and resonance parameters. For this reason we have confined our analysis of the capture data below this energy even though a large number of resonances are seen in the capture measurements up to about 300 keV (Fig. 6). We feel the uncertainties from the analysis of these higher energy resonances in the capture data would be too large for the data to be meaningful. Hence, above 130 keV we have determined values of the average capture cross sections which may be needed for reactor applications. These data are listed in Table VII.

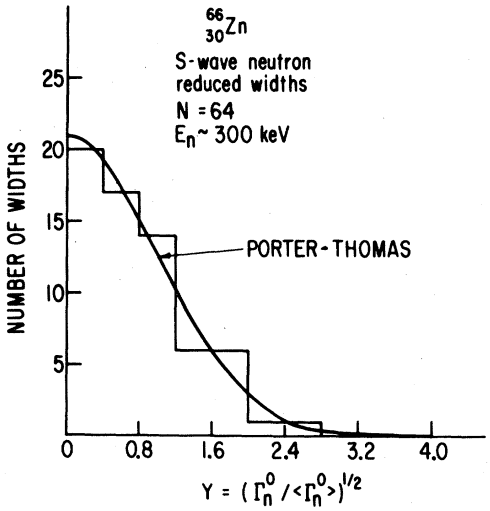

FIG. 7. Reduced neutron width distribution for s-wave resonances of (^{66}Zn+n). The curve is the Porter-Thomas distribution.

DISTRIBUTION OF NEUTRON REDUCED WIDTHS FOR P-WAVE RESONANCES

An investigation of the distribution of reduced neutron widths for p-wave resonances as observed in the transmission measurements up to 130 keV was made. A comparison of this distribution with the Porter-Thomas curve showed that there is a

TABLE VII. The average capture cross section as a function of neutron energy interval. The data has been corrected for the normalization error of 0.95 (see Ref. 18).

E_n(keV)	$\sigma_{n\gamma}$(mb)	E_n(keV)	$\sigma_{n\gamma}$(mb)
3-6	70.45	200-220	19.77
6-9	35.94	220-240	17.97
9-12	92.88	240-260	17.30
12-15	108.86	260-280	16.26
15-20	62.8	280-300	16.73
20-30	41.07	300-320	17.02
30-40	22.34	320-340	16.92
40-50	43.07	340-360	15.69
50-60	26.14	360-380	15.69
60-80	27.00	380-400	16.73
80-100	22.34	400-420	18.63
100-120	16.26	420-440	17.21
120-140	23.58	440-460	18.16
140-160	22.63	460-480	18.63
160-180	21.68	480-500	17.87
180-200	20.54		

significant lack of narrow widths in the data. This effect, as was discussed earlier, is due to our inability to observe very narrow resonances in the transmission measurements. Hence, the resonances observed in the combined measurements of transmission and capture were investigated. The histogram plot of the neutron reduced widths of all observed $\ell>0$ resonances is shown in Fig. 8. A comparison of these data with the Porter-Thomas curves normalized for 154 and 104 resonances are shown as A and B in the figure. The curve B, which shows a good agreement with the data for $(g\Gamma_n^1)^{1/2} > 0.4$ $(eV)^{1/2}$ indicates that there is an excess of many narrow widths in the data. This fact suggests that many of these narrow resonances are probably d wave and that we are able to observe in the capture measurements almost all the p-wave resonances including the narrowest ones.

To assign the excess resonances as d-wave, we have used Bayes' theorem of conditional probability as discussed in an earlier publication.[6] Assuming values of $S_1 = 0.66 \times 10^{-4}$, $S_2 = 0.6 \times 10^{-4}$ and $D_1 = 1.17$ keV as obtained from these measurements, we find that 43 of the narrowest resonances have probabilities of 50% or greater of being d wave. These are indicated in Table V. This is obviously an oversimplification of this problem, since some of these narrow resonances could be p-wave and some of the broader resonances could be d wave; however, in the absence of any better criterion such as parity determination, this appears to be a reasonable assumption. A Monte Carlo analysis gives a value of $\nu = 1.15^{+0.15}_{-0.25}$ for this set of p-wave resonance widths, which is again in excellent agreement with the Porter-Thomas prediction.

DISTRIBUTIONS OF NEUTRON REDUCED WIDTHS FOR D-WAVE RESONANCES

The d-wave neutron capture by an even-even target nucleus (I=0) populates resonances with $J^\pi = 3/2^+$ and $5/2^+$. Applying the level density formula given later in Eq. (1) along with the experimental value of mean spacing $D_0 = 4.62$ keV obtained for s-wave resonances, a value for the mean d-wave level spacing $D_2 = 1.24$ keV is obtained. This corresponds to 105 d-wave resonances up to 130 keV energy. From an analysis of Bayes' theorem we have observed 43 resonances for which the probability for d wave is 50% or larger. An analysis of the neutron reduced width distribution of p-wave resonances shows an excess of about the same number of resonances.

A plot of the distribution of these 43 d-wave neutron reduced widths as a function of $(g\Gamma_n^2)^{1/2}$ is shown in Fig. 9. This histogram is then compared with the Porter-Thomas distribution, which shows a lack of very narrow widths. When the experimental histogram is compared with the Porter-Thomas distribution normalized for 105 resonances, we obtain a good agreement with the experimental data for $\sqrt{g\Gamma_n^2}$ values in excess of 0.7 $eV^{1/2}$; however, there is a

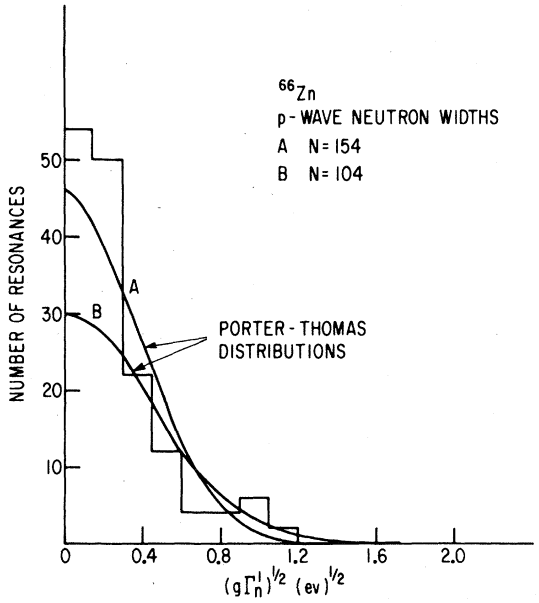

FIG. 8. The neutron reduced width amplitude distribution for 154 p-wave resonances observed up to 130 keV. Theoretical Porter-Thomas distributions normalized for 154 (curve A) and for 104 (curve B) are shown for comparison with the data (histogram).

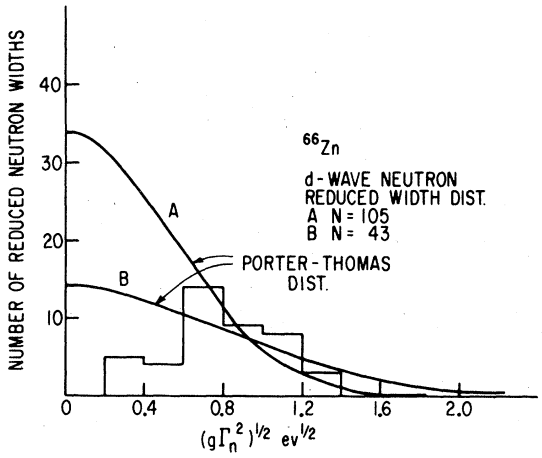

FIG. 9. The neutron reduced width amplitude distribution for 43 d-wave resonances in ^{66}Zn+n. Porter-Thomas distribution curves normalized for 105 widths (curve A) and for 43 widths (curve B) are shown for comparison. This figure permits us to calculate the strengths of missed levels. The number (105) of d-wave resonances up to 130 keV was determined using the level density formula and the measured value of $D_0 = 4.62$ keV.

serious lack of reduced widths smaller than this value. This effect is consistent with what is expected from the sensitivity of even the capture experiments for not being able to observe extremely narrow d-wave widths. However, the fact that we have observed about 40% of the d-wave resonances in these experiments is very impressive; it would be possible to observe more of these widths, if the resolution of the capture measurement were significantly improved.

LEVEL SPACING DISTRIBUTION

The statisical behavior of spacings of complex states with the same J^{π} has been predicted by theoretical calculations based on an orthogonal ensemble of real symmetric matrices of the interaction Hamiltonian. The use of real symmetric matrices in a random model gives the so-called Wigner distribution[3] for the level spacings of same J^{π} as:

$$P(x)dx = \frac{\pi}{2} x\, e^{-\frac{\pi x^2}{4}}, \quad \text{where } x = S/\langle S\rangle .$$

This theory also predicts a value of short range linear correlation coefficient of about -0.27 between adjacent spacings.

The distribution of nearest neighbor level spacings for 64 s-wave resonances observed up to 300 keV has been plotted in Fig. 10. The theoretical Wigner curve is also shown for comparison. The experimental distribution (histogram) shows a small probability for small spacings as predicted by the theoretical distribution.

The number of s-wave resonances observed vs neutron energy is shown in Fig. 11. This shows a straight line up to the maximum energy of 380 keV, indicative of no significant loss of s-wave levels, provided one assumes that no increase in the number of levels is expected in the entire energy interval up to 380 keV. As discussed in the following section on level density the number of levels should increase by about 10% in each interval of 100 keV. Consequently one should expect the slope of the curve through the data points in Fig. 11 to increase as a function of neutron energy. The fact that one observes a nearly straight line may be either an indication of the loss of levels at higher energies, say above 150 keV, or it could be due to a random uncertainty associated with a small number of observed resonances according to Table VIII. One observes 21 certain s-wave resonances which has a random uncertainty of $\sqrt{21}$ = 4.5 resonances, whereas if these levels obey the Wigner distribution, the uncertainty would be $\sqrt{0.27/N}$ or about 2 resonances.[13] In the energy interval 100-200 keV we observed 19 certain s-wave resonances, which is 2 levels or 10% smaller than in the first energy interval, whereas we would expect to have observed an excess of 2 levels. Similarly for the interval 200-300 keV we expected a further excess of 2 levels over the number found in the energy interval 100-200 keV, whereas we observed experimentally 22 levels or an excess of 3 resonances as compared to the previous interval. However, the inconsistency with the original choice of 21 certain s-wave levels in the 0-100 keV energy interval still remains.

Our conclusion on the experimental behavior of Fig. 11 is that the number of observed resonances (21) in a given energy interval (0-100) keV is too small to make any definitive conclusions either on the validity of the level density formula or on the missing of levels in the subsequent energy intervals. These numbers are within the statistical uncertainty as explained.

The Δ_3 statistic as discussed by Dyson

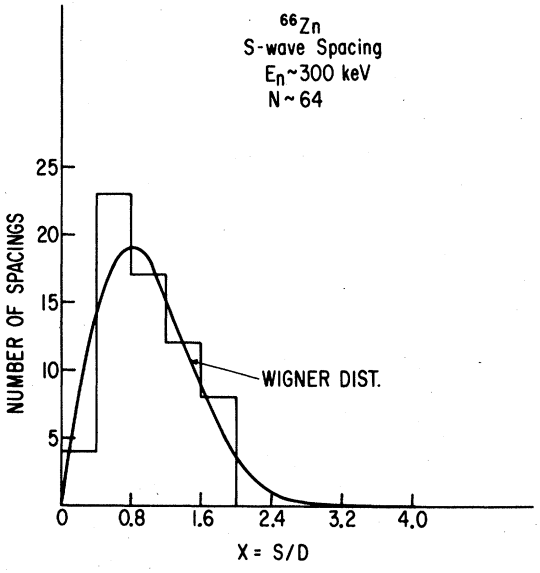

FIG. 10. The distribution of the nearest neighbor spacings of 64 s-wave resonances observed up to E_n ~ 300 keV. The solid curve is the Wigner distribution.

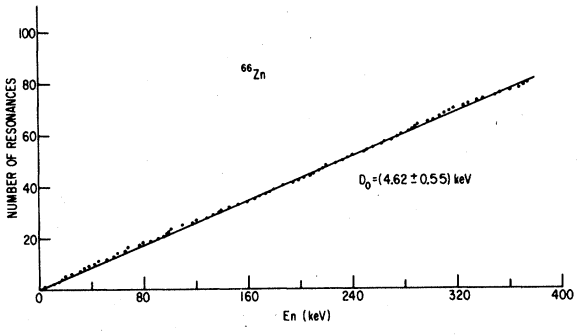

FIG. 11. A cumulative plot of the number of s-wave resonances observed as a function of neutron energy. The slope of the straight line passing through the points can give an estimate of mean level spacings.

TABLE VIII. The number of resonances observed, mean level spacing, nearest neighbor spacing correlation, Δ_3 values (experimental and theoretical) for s-wave resonances as a function of neutron energy interval. The last row of the table gives the values of these quantities if the 3 doubtful levels are eliminated from the analysis. The numbers in parentheses in column 2 are the number of observed levels if doubtful levels are eliminated.

Energy range (keV)	No. of resonances observed	Mean level spacing D in keV	Correlation coefficient	Δ_3 Exp.	Δ_3 Theory
0-100	23 (21)	4.54 ± 0.50	-0.28	0.23	0.31
0-200	43 (40)	4.65 ± 0.37	-0.03	0.47	0.37
0-300	65 (62)	4.62 ± 0.30	-0.07	0.48	0.42
0-375	80 (77)	4.68 ± 0.28	-0.10	0.57	0.44
0-300	(62)	4.84 ± 0.32	-0.05	0.52	0.42

and Mehta[14] can be a sensitive test of the long range correlations between level spacings. This statistic is a measure of the mean square deviation of a staircase plot of a sequence of n levels from a best fitting straight line. Dyson and Mehta[14] have calculated the expected behavior of Δ_3 and its standard deviation for a single population of n levels of the same J^π. They find that:

$$\langle\Delta_3\rangle = \frac{1}{\pi^2}\,[\ell n(n) - 0.0687]$$

with a standard deviation of 0.11. For a two-level sequence the values of $\langle\Delta_3\rangle$ would be twice as large.

The fractional uncertainty in $\langle D\rangle$ due to Dyson-Mehta's Δ_3 statistic is given as

$$\frac{0.45}{N}\,[\ell n\,(2\pi N) + 0.343]^{1/2},$$

which for 20 resonances is about 5% as compared to about 12% for Wigner distribution and 22% for the purely random distribution.

We have calculated the value of Δ_3 for s-wave resonances as a function of neutron energy and the results for a few energy intervals are given in Table VIII. The experimental value of 0.48 up to 300 keV is in excellent agreement with the theoretical value of (0.42 ± 0.11). The values obtained for other energy intervals such as 0-100 keV, 0-200 keV are also in excellent agreement.

The resonances at 31.020, 59.580 and 194.485 keV have doubtful parity assignments since these do not show the asymmetric resonance shape clearly. If we calculate the Δ_3 value after eliminating these resonances, we obtain a value of 0.52 up to 300 keV, again in very good agreement with the theoretical value. Thus, in this case, the presence or absence of these doubtful resonances from the level sequence provides equally acceptable values of Δ_3. The value -0.28 found for the correlation coefficient between nearest neighbor spacings up to the energy of 100 keV is in excellent agreement with the predicted value of -0.27 of the random-matrix model; however, it decreases to a value of -0.10 for the maximum energy of 380 keV, indicative of some impurity in the level sequence. The mean value of D_o = (4.62 ± 0.55) keV is about 12 times the instrumental energy resolution of about 0.38 keV at the highest energy of 300 keV used for the statistical analyses. Thus, we feel that the data on the s-wave spacing distribution in the interval $0<x<0.4$ should be fairly accurate.

A similar investigation of distribution of 154 spacings for $\ell>0$ resonances up to $E_n \sim 130$ keV is shown in Fig. 12 along with the Wigner distribution for two merged p-wave sequences. The agreement is good for large values of x but the data show an excess of small spacings. One should not, however, expect a good agreement since there are at least 43 of these resonances which have been assigned as d wave from the analysis of p-wave neutron reduced width distribution and from Bayes' theorem. However, the exact location of these resonances is not precisely known. Assuming that 43 resonances out of 154 are d wave, one obtains a value for mean spacing for p-wave levels of (1.17 ± 0.14) keV. The uncertainty for a merged sequence of two spins is calculated from the relation $\Delta D = D\sqrt{0.54/N}$ plus the uncertainty due to the increase in level density as a function of energy.

LEVEL DENSITY

Level densities of complex states have been a subject of investigation for many decades. A good basis for the computation of these level densities has been the independent particle model. The single particle energy levels in the average potential field are, in general, used to determine possible configurations of nucleons in unoccupied states and thus to generate the higher energy complex states.

The application of these simple ideas produces two striking effects: (1) the level density in general increases exponentially

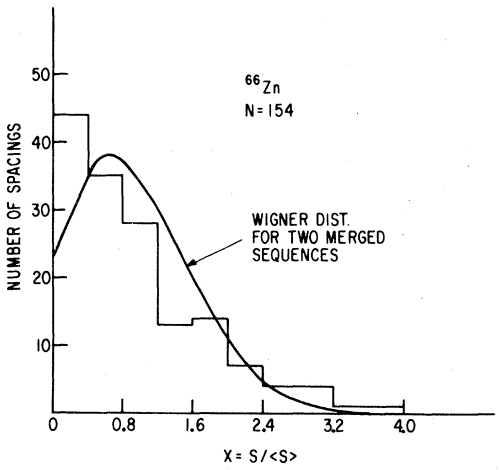

FIG. 12. The distribution of the nearest neighbor spacings of 154 $\ell>0$ resonances observed up to 130 keV. The solid curve is the Wigner distribution for two merged sequences of $J^\pi = 1/2^-$ and $3/2^-$ with equal mean spacings.

with the excitation energy in view of the many possible configurations in the higher excited states, and (2) the total angular momentum J of the states plays an important role using the Fermi-gas model as a starting point. The level density for a given spin as a function of the excitation energy U can be given as[15]

$$\rho(U) = \{\sqrt{48}\ U'\}^{-1} \exp 2\sqrt{aU'},$$

where U' is the effective excitation energy corrected for odd-even effect and is given as

$$U' = U + \delta$$

where δ is the pairing energy, and a is the level density parameter. Using the value[16] of a = 10 MeV^{-1}, δ = 1.06 MeV and B_n = 7.053 MeV for ^{66}Zn, we have determined the increase in level density in the energy intervals 100-200 keV and 200-300 keV, using the midenergy point for calculation. The expected increase has been discussed in a previous section.

The level density as a function of J at a given energy of excitation can be given as[15]

$$\rho_J(U) = \rho_o(U)(2J+1)\exp\left[-\frac{(J+1/2)^2}{2\sigma^2}\right] . \quad (1)$$

Here σ is the cut-off parameter and is related to the moment of inertia of the nucleus. The value of σ^2 is slightly dependent on mass and energy. For Zn nuclei its value is about 10. This simple expression for J dependence of level density may be subject to question for large values of J but is shown to be valid for small values of J as is the case here. It is possible to test the validity of this relationship from the present results of level density values obtained for different angular momenta (J) and parity (π) of resonances. Since ^{66}Zn is an even-even nucleus with spin I = 0, compound states of only $J^\pi = 1/2^+$ are populated by neutron capture in s-wave resonances. A value of D_o of (4.62 ± 0.55) keV for s-wave resonances at neutron binding energy has been determined from this experiment. The resonances populated by p-wave neutrons have $J^\pi = 1/2^-$ and $3/2^-$. Since it is not possible to make a definite assignment of spins for the p-wave resonances, one can only obtain an average value for the p-wave level spacing. This has been determined to be D_1 = (1.17 ± 0.14) keV from this experiment.

The ratio of level densities for p- and s-wave resonances can be thus obtained from the formula using a value of $\sigma^2 \sim 10$ for this mass region.[16] This value for ^{66}Zn is 2.72. The experimental value is $3.95^{+1.06}_{-0.84}$, indicating that there are perhaps more negative parity states than the positive parity states at the excitation energy corresponding to the neutron binding energy. Before accepting this conclusion a certain amount of discussion is needed.

Even though it is impossible to be certain that the correct parity assignments of all the observed resonances have been made, and that no resonances have been missed in the energy interval considered, we feel that a combination of the use of correct formalism of resonance analysis, such as R matrix used here and the application of statistical distribution of level spacings and neutron reduced widths should provide a reasonable basis that these results are accurate within at least 10%. One should note that the ambiguity between s- and p-wave resonances is less than between p- and d-wave since for the latter, we have used the Bayes theorem for assigning d-wave resonances. If all the observed resonances were p wave, it would provide a larger discrepancy from the 2J+1 law, hence, we must be observing some d-wave levels up to 130 keV which is a clear evidence of the observation of d-wave resonances at low neutron energies in medium weight nuclei. The probability that a much larger number of narrow resonances observed are d wave is small due to low penetrability at these energies and would be inconsistent with the p-wave neutron width distribution.

Calculations of Soloviev[17] do indicate the possibility of a parity dependence of level density in even-even nuclei. His calculations for ^{54}Fe show that there are more $1/2^-$ states than $1/2^+$. Data from the present experiments on d-wave resonances with $J^\pi = 3/2^+, 5/2^+$ appear to suggest such an effect.

s- and p-WAVE STRENGTH FUNCTIONS

The cumulative sum of Γ_n^o vs neutron energy for the observed s-wave resonances has been plotted in Fig. 13. If all the points pass through a straight line, the slope of the straight line can provide a value for the strength function. It can, however, be seen from Fig. 13 that the

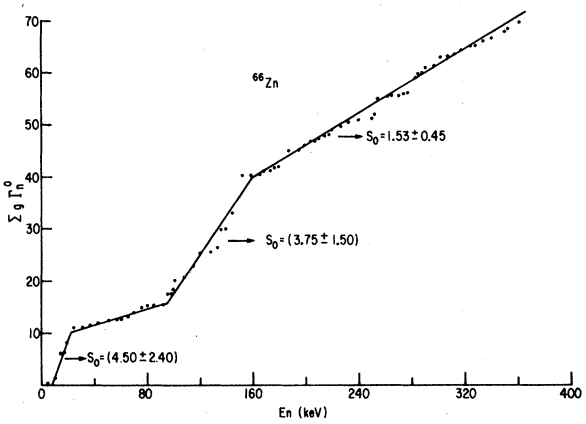

FIG. 13. A cumulative plot of the sum of the s-wave neutron reduced widths as a function of neutron energy. The solid curves are drawn through all the points in a given energy interval. The slopes of these straight lines can provide the values of s-wave strength function.

points from 0 to 25 keV lie on one slope, but those from 25-100 keV, 100-160 keV and 160-360 keV lie on different slopes, giving different values of the s-wave strength function. We have calculated these values for different energy intervals using the relation $S_o = \Sigma\Gamma_n/\Delta E$. These are given in Table IX. From these we choose the overall value $S_o = 2.06 \pm 0.36$ in units of 10^{-4} $eV^{-1/2}$.

A large value of $S_o(10^4) = (4.50 \pm 2.40)$ is observed up to 25 keV, which may indicate the presence of an intermediate state at about this energy. A similar sharp step is observed at $E_n \sim 140$ keV giving $S_o = (3.75 \pm 1.50)$; however, both these values are within the statistical uncertainties of the chosen value. Hence, the interpretation of these as doorway states at these energies needs to be proven by other tests. A similar plot for the p-wave resonances is shown in Fig. 14. It shows a straight line up to $E_n \sim 290$ keV passing through most of the points. At about 293 keV, there is a big step rise and then it smooths out again after about 300 keV. This step is an indication of an intermediate state in the p-wave resonances. The values of p-wave strength function for a few energy intervals are given in Table IX. From these we chose the final value of $S_1(10^4) = (0.66 \pm 0.06)$. For this determination a value of nuclear radius R = 5.6 fm was used.

d-WAVE STRENGTH FUNCTION

As discussed earlier we have observed 43 d-wave resonances up to 130 keV in the capture cross section data. From these we can calculate the d-wave strength function S_2 which for 43 resonances and a radius of 5.6 fm is equal to $(0.40 \pm 0.08) \times 10^{-4}$. The forty three resonances constitute about 40% of the resonances expected in this energy interval, however these resonances most likely have the largest widths and thus contribute most to the strength function. The correction needed for the missed resonances can be calculated from an examination of Fig. 9. This constitutes a correction of about 25% to the strength, thus giving the final value of $S_2 = (0.50 \pm 0.12) \times 10^{-4}$.

TABLE IX. s- and p-wave neutron strength function values for different neutron energy intervals.

Energy interval (keV)	Strength function $S_o \times 10^4$ $eV^{-1/2}$	Strength function $S_1 \times 10^4$ $eV^{-1/2}$
0-25	4.50 ± 2.40	0.76 ± 0.20
0-100	2.00 ± 0.57	0.58 ± 0.09
0-200	2.30 ± 0.49	0.55 ± 0.06
0-300	2.06 ± 0.36	0.66 ± 0.06
100-200	2.61 ± 0.73	0.51 ± 0.08
200-300	1.56 ± 0.45	0.86 ± 0.13

CORRELATION BETWEEN s-WAVE NEUTRON REDUCED WIDTHS AND RADIATION WIDTHS

A large and significant correlation between neutron reduced widths and radiation widths of s-wave resonances has been previously observed for some nuclei in this mass region. Similarly a large correlation between (n,γ) partial widths and (d,p) spectroscopic factors has been observed in some nuclei.

We have investigated 26 s-wave resonances in ^{66}Zn and find a value of $\rho = 0.59 \pm 0.10$ for the correlation between neutron reduced widths and radiation widths. This is a large and significant value and indicates that the radiative decay process via s-wave capture in this nucleus is a simple one consisting of only a few transitions to the low lying states in the residual nucleus.

SUMMARY

The neutron total and capture cross sections of the separated isotope ^{66}Zn has been measured for the first time with high resolution up to about 1 MeV and resonance parameters E_o, $g\Gamma_n$, have been measured up to 370 keV and Γ_γ up to 130 keV. From these precise results we have been able to investigate the statistical distributions of nearest-neighbor level spacings and neutron reduced widths. Both of these distributions are found to be in excellent agreement with theory. Moreover, we have found good agreement of the data with the Dyson-Mehta Δ_3 statistics. This agreement is most reliable up to 200 keV neutron energy. Above this energy the agreement could be fortuitious, since firstly the energy resolution of these measurements is such that it inhibits the observation of very weak resonances (Table II). This effect could contribute to a loss of as many as 2 levels between 200-300 keV energy interval. Secondly the level density is increasing as a function of excitation energy by about 9% per 100 keV. Since the graph of number of levels vs E_n (Figure 11) is linear, the loss of levels is almost exactly compensated for by the increase in

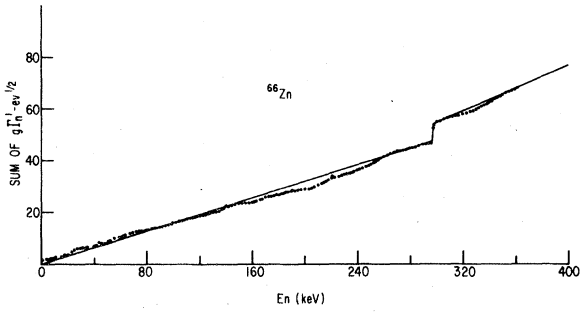

FIG. 14. A cumulative plot of the sum of the p-wave neutron reduced widths as a function of neutron energy. The solid curves are drawn through the points.

level density. Similar situations were present in the investigation of ^{64}Zn nucleus.

We feel, however, that the most important criterion for the assignment of parities for ℓ=0,1 resonances is the resonance shape and not the application of Bayes' theorem or other statistical concepts.

We have also been able to demonstrate that even the highest resolution transmission measurements are not adequate to observe a complete sequence of narrow p-wave resonances and that capture cross section measurements are essential to resolve this shortcoming. We have thus determined a precise value for S_1 and a reasonable value for S_2.

This research was sponsored by the Division of Nuclear Sciences, U.S. Department of Energy, under Contract No. W-7405-eng-26 with the Union Carbide Corporation and Contract No. DE-AC02-76ER02439 with the State University of New York at Albany. One of us (VKT) would like to express his gratitute to the Saha Institute of Nuclear Physics, Calcutta (India) for a leave of absence.

---

[1]C. Porter, H. Feshbach, and V. Weisskopf, Phys. Rev. 96, 448 (1954).
[2]B. Block and H. Feshbach, Ann. Phys. (N.Y.) 23, 47 (1963).
[3]E.P. Wigner, Proc. Gatlinburg Conf. Neutron Time-of-Flight Methods, Oak Ridge National Laboratory Report ORNL-2309 (1957).
[4]C.E. Porter and R.G. Thomas, Phys. Rev. 104, 483 (1956).
[5]J. E. Lynn, Theory of Neutron Resonance Reactions (Clarendon, Oxford, 1968).
[6]J.B. Garg, V.K. Tikku, and J.A. Harvey, Phys. Rev. C 23, 671 (1981); J.B. Garg, V.K. Tikku, J. Halperin and R. Macklin, ibid. 23, 683 (1981).
[7]Neutron Cross Sections, Vol. I, Resonance Parameters, BNL-325, 3rd edition, 1973, edited by S.F. Mughabghab and D.I. Garber.
[8]M.S. Pandey, J.B. Garg, and J.A. Harvey, Phys. Rev. C 15, 600 (1977).
[9]R.L. Macklin and B.J. Allen, Nucl. Instrum. Methods 91, 565 (1971).
[10]R.L. Macklin, Nucl. Instrum. Methods 91, 79 (1971).
[11]B.J. Allen, R.L. Macklin, R.R. Winters, and C.Y. Fu, Phys. Rev. C 8, 1504 (1973).
[12]G.F. Auchampaugh (private communication).
[13]E. Lynn, The Theory of Neutron Resonance Reactions (Clarendon, Oxford, 1968), p. 108.
[14]F.J. Dyson, J. Math. Phys. 3, 140, 157, 166, 1199 (1962), F.J. Dyson and M.L. Mehta, ibid 4, 701 (1963).
[15]J.R. Huizenga and L.G. Moretto, Annu. Rev. Nucl. Sci. 22, 427 (1972).
[16]H. Baba, Nucl. Phys. A159, No. 2, 625 (1970).
[17]V.G. Soloviev, Ch. Stoyanov, and A.I. Vdovin, Joint Inst. Nucl. Res. Report P4-7499, Dubna, 1973.
[18]R.L. Macklin and R.R. Winters, Nucl. Sci. Eng. 78, 110 (1981).